
**ELECTRICAL
AND MAGNETIC PROPERTIES**

Magnetic States and Hysteresis Properties of Small Magnetite Particles

L. L. Afremov and A. V. Panov

Far East State University, ul. Sukhanova 8, Vladivostok, 690600 Russia

Received March 24, 1998

Abstract—Ground and metastable states of magnetite grains of near-single-domain size are considered in terms of a model developed by the authors. The grains are shown to exist, depending on their size and prolateness, in one of three magnetic states, namely, with uniform magnetization, weakly nonuniform magnetization (quasi-single-domain state), and strongly nonuniform magnetization (two-domain state). Critical sizes for the uniform and quasi-single-domain states are calculated. Magnetization reversal of such grains is simulated. The coercive force and critical field are studied as functions of the size and prolateness of the grains and the direction of the applied magnetic field. A significant feature distinguishing the results of this work from other similar studies is the nonmonotonic behavior of the coercive force of a particle with an increase in its prolateness.

INTRODUCTION

The magnetic properties of small ferromagnetic particles were studied in numerous (predominantly theoretical) investigations [1–10], in which the authors proceeded from some assumptions about the magnetization distribution. These models either use a variational procedure to minimize the total energy or solve the Landau–Lifshitz equation. Progress in computer engineering made it possible to pass from the simple model [1] representing the domains and domain walls as uniformly magnetized parallelepipeds to models with a three-dimensional distribution of magnetization [3, 5, 6].

However, none of these studies could claim a comprehensive consideration of the problem, as they were aimed at solving particular, specified problems. In spite of the advantage of three-dimensional models due to an increase in the number of degrees of freedom, the numeric solutions still stay approximate. The accuracy of a solution depends on the partitioning method (computer facilities), and it is this that determines the class of minimizing functions. Magnetization distributions obtained in [3, 5, 6] correspond to the chosen classes of functions. Therefore, it is difficult to evaluate the advantages of the conclusions based on the approximate solutions of three-dimensional models over the results obtained in terms of two-dimensional simulation. For example, a simplifying assumption on the strictly antiparallel orientation of domain magnetic moments used [1, 4] restricted the possibility of studying the effects of an applied magnetic field on the magnetization distribution in grains. Investigations of magnetization of the particles [6, 8, 9] performed in terms

of three-dimensional models, used the assumption that the magnetocrystalline anisotropy is uniaxial.

In this work, we studied the process of magnetization of small magnetite grains of various sizes and prolateness.

1. THE MODEL OF A PARTICLE UNDER STUDY

Let us consider a grain of a mineral with a cubic structure. Let it be a rectangular parallelepiped with a base of area a^2 and a height qa (cube edges are coincident with the crystallographic axes). We restrict the consideration to the case where the magnetic moment is distributed in the yOz plane (Fig. 1) as follows:

$$\theta(x) = \begin{cases} \theta_1, & 0 \leq x \leq p_1, \\ \theta_1 + \frac{(\theta_2 - \theta_1)}{p_2}(x - p_1), & p_1 \leq x \leq p_1 + p_2, \\ \theta_2, & p_1 + p_2 \leq x \leq 1, \end{cases} \quad (1)$$

where θ_1 and θ_2 are the angles between the magnetic moment and the Oz axis in the first and in the second domains, respectively; p_1 and p_2 are the widths of the domain and the domain wall, respectively; and the variables x , y , and z are normalized to a .

Investigation of the equilibrium states of the magnetic moment of the grain is performed by minimizing its total energy E with respect to four parameters θ_1 , θ_2 , p_1 , and p_2 . (Equations for reduced energy $\varepsilon = \frac{E}{qa^3 I_s^2}$ are used below).

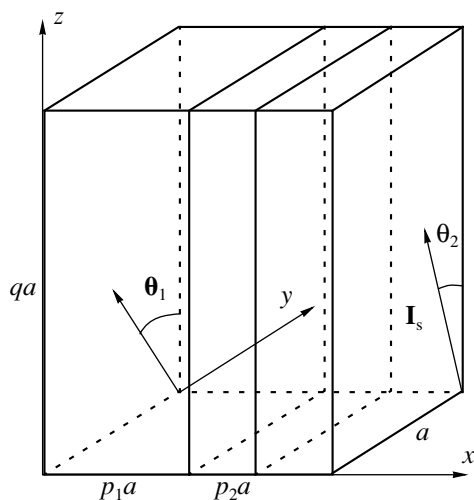


Fig. 1. A schematic of the model.

The total energy of the grain magnetic moment includes exchange energy

$$\epsilon_{\text{ex}} = A \frac{(\theta_2 - \theta_1)^2}{p_2 a^2 I_s^2}, \quad (2)$$

energy of magnetocrystalline anisotropy

$$\epsilon_{\text{an}} = \frac{K}{8I_s^2} \left\{ 1 - p_1 \cos 4\theta_1 - (1 - p_1 - p_2) \cos 4\theta_2 - \frac{p_2 (\sin 4\theta_2 - \sin 4\theta_1)}{4(\theta_2 - \theta_1)} \right\}, \quad (3)$$

magnetostatic energy

$$\begin{aligned} \epsilon_{\text{m}} &= \frac{1}{2qa^3 I_s^2} \iint_{S,S'} \frac{(\mathbf{I}_s(\mathbf{r}), d\mathbf{s})(\mathbf{I}_s(\mathbf{r}'), d\mathbf{s}')}{|\mathbf{r} - \mathbf{r}'|} \\ &= \frac{1}{q} \int_0^1 dx \int_0^1 dx' \{ f_1(x-x') \cos \theta(x) \cos \theta(x') \\ &\quad + f_2(x-x') \sin \theta(x) \sin \theta(x') \}, \end{aligned} \quad (4)$$

and the energy of the magnetic moment in an applied magnetic field \mathbf{H}

$$\epsilon_H = -\frac{1}{qa^3 I_s^2} \int (\mathbf{H}, \mathbf{I}_s) dV = -\frac{Hm(\theta_1, \theta_2, p_1, p_2, \varphi)}{I_s}. \quad (5)$$

The following designations are assumed: A is the exchange constant; \mathbf{I}_s is the spontaneous magnetization vector, whose magnitude is uniform over the grain volume V ; K is the constant of magnetocrystalline anisotropy;

ds is a surface element; φ is the angle between the \mathbf{H} vector and the Oz axis;

$$\begin{aligned} f_1(\tau) &= q \ln \left\{ \frac{(\sqrt{q^2 + \tau^2} + q) \sqrt{1 + \tau^2}}{(\sqrt{1 + q^2 + \tau^2} + q) |\tau|} \right\} \\ &\quad - \sqrt{q^2 + \tau^2} + \sqrt{1 + q^2 + \tau^2} - \sqrt{1 + \tau^2} + |\tau|, \end{aligned} \quad (6)$$

$$\begin{aligned} f_2(\tau) &= \ln \left\{ \frac{(\sqrt{1 + \tau^2} + 1) \sqrt{q^2 + \tau^2}}{(\sqrt{1 + q^2 + \tau^2} + 1) |\tau|} \right\} \\ &\quad - \sqrt{1 + \tau^2} + \sqrt{1 + q^2 + \tau^2} - \sqrt{q^2 + \tau^2} + |\tau|, \\ &\quad m(\theta_1, \theta_2, p_1, p_2, \varphi) \end{aligned}$$

$$\begin{aligned} &= \left\{ p_1 \cos(\theta_1 - \varphi) + (1 - p_1 - p_2) \cos(\theta_2 - \varphi) \right. \\ &\quad \left. + \frac{p_2 [\sin(\theta_2 - \varphi) - \sin(\theta_1 - \varphi)]}{\theta_2 - \theta_1} \right\}, \end{aligned} \quad (7)$$

where $m(\theta_1, \theta_2, p_1, p_2, \varphi)$ is the projection of the magnetic moment onto the direction specified by the \mathbf{H} vector, normalized to $qa^3 I_s$.

A step-by-step minimization procedure was used. At first, a minimum was found near a specified point. The obtained point was used as the starting point for the next iteration. The minimization procedure was interrupted when the energy at the new starting point turned out to be lower than in neighboring points. The accuracy of the calculations was limited by the step value ($\Delta p = 6 \times 10^{-3}$, $\Delta \theta = 6 \times 10^{-3}$ rad) and by the computing accuracy (the comparing energies in two neighboring points). When calculating hysteresis loops, an energy minimum was searched for, and the projection of the magnetic moment onto the applied-field direction was calculated for the obtained values of θ_1 , θ_2 , p_1 , and p_2 . The magnetic field was varied in steps of $\Delta H = 10$ Oe.

The model suggested is a further development of the model of Shcherbakov *et al.* [4], in which the antiparallel orientation of the magnetic moments of domains is fixed.

2. GROUND AND METASTABLE STATES

Simulating the magnetization distribution in magnetite grains ($I_s = 485$ Oe, $A = 1.32 \times 10^{-6}$ erg/cm, $K = -1.36 \times 10^5$ erg/cm³) of various sizes and prolateness performed at $\mathbf{H} = 0$ distinguished three types of magnetic states:

- uniform-magnetization states;
- states with a weak nonuniformity of I_s (quasi-single-domain state);
- states with a strong nonuniformity of the magnetic moment (two-domain state).

Uniform-Magnetization States

The state with a uniform I_s vector is ground state only in a size range limited from above by the single-domain size a_0 , which exhibits a nonmonotonic behavior with increasing grain prolateness; it decreases from 100 nm for equiaxed particles to 80 nm for particles with the length-to-width ratio $q = 1.3$, and achieves 200 nm for $q = 3.0$ (Fig. 2).

At $a > a_0$, a two-domain or a quasi-single-domain states are more favorable energetically. The uniform state, if it exists, is metastable up to the maximum single-domain size a_{0m} . The a_{0m} dependence on the grain prolateness is shown in Fig. 2. The a_{0m} value is halved with increasing aspect ratio from $q = 1$ to $q = 1.3$, then it increases, and at $q > 3.1$ the uniform distribution of magnetic moment can be realized in particles of any size (Fig. 2).

Nonuniform-Magnetization States

The states with a weakly nonuniform I_s distribution ($|\theta_1 - \theta_2| \sim 30^\circ - 100^\circ$, $0.75 < m < 1$) are only equilibrium within the range $a_0 < a < a_1$ (Fig. 2); and at $a_1 < a < a_{1m}$ they are metastable (a_1 is here the quasi-single-domain size, and a_{1m} is the maximum quasi-single-domain size). Note that at $q > 2.1$ the quasi-single-domain state can be realized in particles of any size exceeding a_1 .

Note also that the range of nonuniformity of the magnetic moment (domain-wall thickness) varies only slightly with increasing grain size and occupies about 2/3 of the total volume.

3. CONSIDERATION OF CALCULATED CRITICAL SIZES

Single-Domain Grain Size

Sizes of the single-domain grains calculated in this work (Fig. 2) are in general agreement with single-domain sizes given in [11] and exceed values obtained by Fabian *et al.* [5]. Note for comparison that the experimentally determined single-domain grain size of a cubic particle is equal to 50 nm according to [12] and to 80 nm according to [13]. Theoretical estimations of a_0 give 80 nm [2, 4] and 100 nm [3]. According to [2, 14], a_0 increases from 80 to 120 nm with increasing grain prolateness from 1 to 2.5.

An important feature of the results obtained in this work is the nonmonotonic behavior of the single-domain size as a function of grain prolateness (Fig. 2). Such an $a_0(q)$ dependence is due to the nonmonotonic behavior of the effective anisotropy constant, which is a results of tensor summation of constants of magnetocrystalline anisotropy and shape anisotropy [15, 16].

Figure 3 displays the orientation of the grain magnetic moment in the uniform state as a function of the aspect ratio q . Competition of different anisotropies results in changing the orientation of the easy axis [15, 16], which can explain the dependence of the crit-

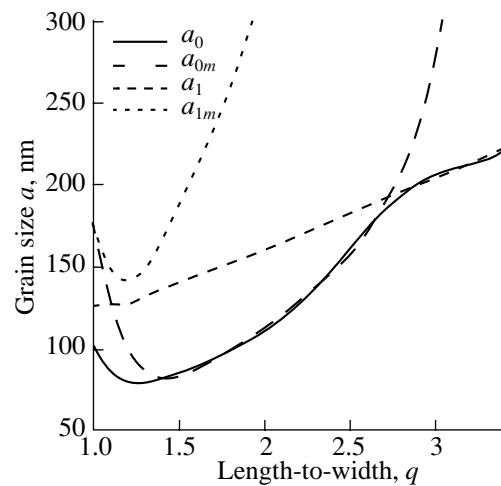


Fig. 2. Single-domain grain size a_0 , maximum size of grains with the uniform distribution of magnetization a_{0m} , quasi-single-domain grain size a_1 , and maximum quasi-single-domain grain size a_{1m} as functions of the grain prolateness (ratio) q .

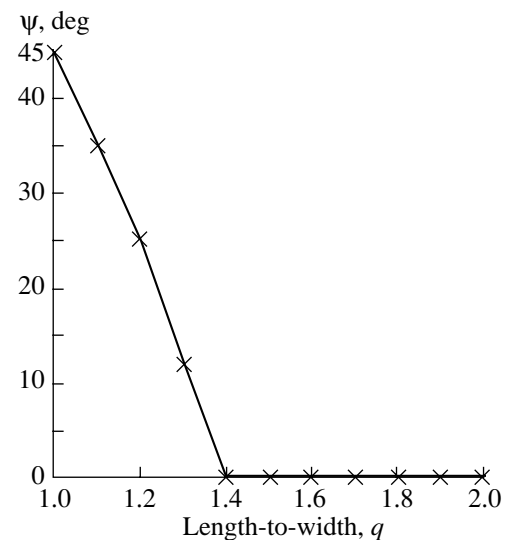


Fig. 3. Angle ψ between the easy axis and the longer edge of a grain as a function of the grain prolateness q .

ical sizes on grain prolateness shown in Fig. 2. Note that the orientation of the easy axis of an equiaxed particle along its face diagonal (rather than along the body diagonal of the cube) is attributed to the restrictions of the model used (the magnetic moment may rotate only in the xOy plane).

Metastable Single-Domain State

The maximum size a_{0m} of a grain in the state with a uniform distribution of I_s qualitatively follows the nonmonotonic behavior of the effective anisotropy constant.

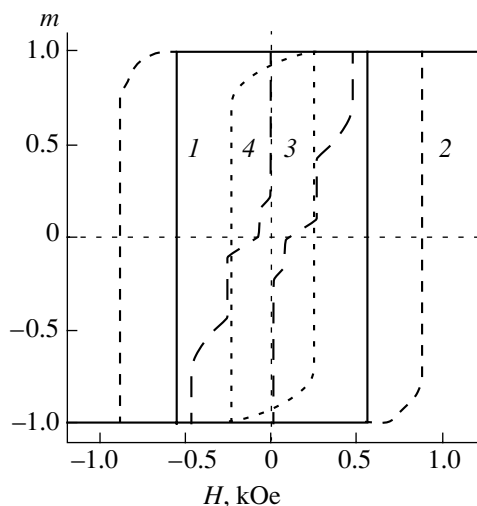


Fig. 4. Hysteresis loops of magnetite particles depending on grain size and length-to-width ratio: (1) $q = 1$, $a = 60$ nm; (2) $q = 2$, $a = 60$ nm; (3) $q = 1$, $a = 180$ nm; and (4) $q = 2$, $a = 180$ nm; m is the relative magnetic moment.

So, the a_{0m} values obtained for slightly elongated particles are close to those given in [2, 4], while for $q > 1.2$, when the shape-anisotropy energy of a magnetite grain becomes comparable with the magnetocrystalline anisotropy energy, the $a_{0m}(q)$ dependence obtained by Shcherbakov *et al.* [4] differs significantly from that calculated in this work. The prolateness at which the maximum size a_{0m} becomes infinite is shifted to larger q values (from 2.2 [4] to 3.1), which results in a significant decrease in a_{0m} in the range $1.2 < q < 3.0$.

Weakly Nonuniform State

The state with a weakly nonuniform magnetic-moment distribution may be identified with both the quasi-single-domain state, or “twisting” mode [17, 18, 19], and a state characterized by the “curling” mode [4, 20]. Unlike the states mentioned above [4, 17, 20], this can be realized along with the “uniform” or the “two-domain state”, remaining stable only in a narrow range of sizes $a_0 < a < a_1$. Note that the values given in Fig. 2 differ by a factor of two from the critical size of the “curling” mode ($a = 40$ nm) [20].

Two-Domain State

In the two-domain state, deviation of the θ_1 and θ_2 angles that determine the orientation of magnetic moments in the first and the second domains from 0° and 180° , respectively, is observed with increasing grain size. This finally results in the appearance of a small magnetic moment in the equiaxed particle at $a > 140$ nm. Similar magnetization distribution (the so-called “skirt”) has been studied for larger particles.

According to calculations, the two-domain state is metastable from below, starting from $a = 120$ nm up to

$a = a_1$; at $a > a_1$, the two-domain state is energetically favorable. It coexists with the uniform state (at $a < a_{0m}$) or with the quasi-single-domain state (at $a < a_{1m}$), and becomes the only state in the range of $a > a_{1m}$. The a_{1m} values are somewhat lower than those given in [2, 4], but are qualitatively consistent with them.

4. MAGNETIZATION CURVE

The results of simulating the magnetization process is illustrated in Fig. 4. Here and below, the direction of the applied magnetic field is assumed to be along the easy axis (see Fig. 3), unless otherwise specified. The field value that causes the reversal of the magnetization sign is called the coercive force H_c ; the field values corresponding to the points of inflections in the magnetization curve are the critical fields of rearrangement of the magnetic structure H_{cr} and H_c in this case may not be equal to any of the H_{cr} values.

Let us consider, for example, magnetization reversal of a cubic particle of size $a = 180$ nm. Assume that the particle was magnetized to saturation in a field whose direction makes an angle of 135° with the Oz axis. The particle remains in the uniform state as the field decreases gradually to zero. In a field $H_{cr1} = 10$ Oe (see table), the particle transforms jumpwise to the two-domain state with a projection of the magnetic moment $m = -0.21$ and stays in this state up to $H_{cr2} = 80$ Oe corresponding to the transformation from one two-domain state to another. The increase in the magnetic moment m in the range between the critical fields H_{cr} occurs through gradual changes in the domain-magnetization directions and domain sizes. In a field $H_{cr3} = 260$ Oe, the particle transforms to the next two-domain state with a projection of the magnetic moment $m = 0.43$ and then, at $H_{cr4} = 480$ Oe equal to the saturation field H_{sat} , it transforms to the uniform-magnetization state.

The particles that are in stable uniform or quasi-single-domain states ($a < \max(a_1, a_{0m})$, Fig. 2) exhibit rectangular or close to rectangular hysteresis loops (Fig. 4, curves 1, 3, 4).

Magnetization of grains that are in the two-domain state or in the metastable quasi-single-domain state ($\max(a_1, a_{0m}) < a < a_{1m}$, Fig. 2) occurs through intermediate two-domain states (Fig. 4, curve 3). Magnetization reversal of particles with sizes $a > a_{1m}$ (corresponding to the stable two-domain state) is a nearly reversible process and the coercivity of these particles is almost zero. Thus, the process of magnetization of small grains depends essentially on their magnetic state at $H = 0$.

The grain size and their prolateness significantly affect not only the shape of the hysteresis loop, but also the critical values of critical fields H_{cr} (see table), the coercive force H_c , and the saturation field H_{sat} (Figs. 5, 6). The nonmonotonic behavior of H_c depending on the grain prolateness q should be noted. The $H_c(q)$ curve qualitatively follows the dependence of the maximum size of the quasi-single-domain grains a_{1m} on q , which

Critical fields H_{cr} for magnetite particles of various size a and prolateness q m_{before} and m_{after} are the projections of the magnetic moment onto the H direction before and after transition from one magnetic state to another

a , nm	q	H_{cr} , kOe	m_{before}	m_{after}	a , nm	q	H_{cr} , kOe	m_{before}	m_{after}
60	1	0.57	-1	1	180	1.2	-0.3	-0.996	-0.783
	1.2	0.32	-1	1			-0.1	-0.615	-0.274
	1.4	0.49	-0.636	1			-0.07	-0.245	-0.093
	1.6	0.63	-0.714	1			0.21	0.105	0.342
	1.8	0.76	-0.753	1		0.24	0.442	0.744	
	2	0.88	-0.773	1		0.53	0.938	1	
	2.5	1.11	-0.853	1		1.4	0.01	-0.69	0.005
	3	1.29	-0.886	1			0.17	0.155	0.353
5	1.71	-0.948	1	0.22	0.468		0.85		
100	1	0.41	-1	1	1.6		0.1	-0.715	0.085
	1.2	0.1	-0.999	-0.713		0.19	0.211	0.476	
	2	0.2	-0.554	1		0.2	0.476	0.903	
	1.4	0.45	-0.711	1		1.8	0.18	-0.73	0.227
	1.6	0.55	-0.719	1	0.19		0.227	0.947	
	1.8	0.63	-0.733	1	2		0.25	-0.711	0.996
	2	0.71	-0.724	1	2.5		0.37	-0.786	1
	2.5	0.85	-0.735	1	3	0.48	-0.785	1	
3	0.95	-0.757	1	5	0.72	-0.83	1		
5	1.18	-0.801	1	220	1	0.34	-1	0.393	
140	1	0.12	-1		-0.285	0.36	0.426	0.664	
	2	0.27	-0.178		0.594	0.52	0.854	1	
	3	0.35	-0.725		1	1.2	-0.36	-0.993	-0.783
	1.2	-0.18	-1		-0.779		-0.12	-0.557	-0.064
	2	0.04	-0.576		-0.01		0.25	0.206	0.366
	3	0.07	0.059		0.409		0.43	0.595	0.828
	5	0.16	0.553		0.763	0.62	0.938	1	
	3	0.39	0.922	1	1.4	-0.04	-0.68	-0.029	
1.4	0.14	-0.677	0.875	0.29		0.255	0.504		
1.6	0.23	-0.696	0.958	0.31		0.53	0.855		
1.8	0.31	-0.696	1	1.6		0.05	-0.704	0.036	
2	0.37	-0.746	1		0.29	0.291	0.91		
2.5	0.51	-0.772	1		1.8	0.13	-0.72	0.123	
3	0.62	-0.764	1			0.28	0.299	0.955	
5	0.85	-0.832	1	2		0.21	-0.702	0.237	
180	1	0.01	-1	-0.211		0.28	0.322	0.987	
	2	0.08	-0.156	-0.007	2.5	0.29	-0.807	1	
	3	0.26	0.089	0.434		3	0.1	-0.999	-0.986
	5	0.48	0.686	1		0.41	-0.805	1	
5	0.65	-0.833	1	5		0.65	-0.833	1	

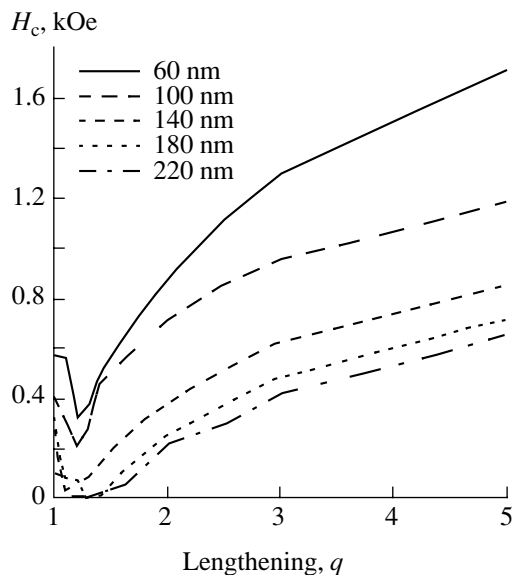


Fig. 5. Coercive force H_c of magnetite particles as a function of their length-to-width ratio and size.

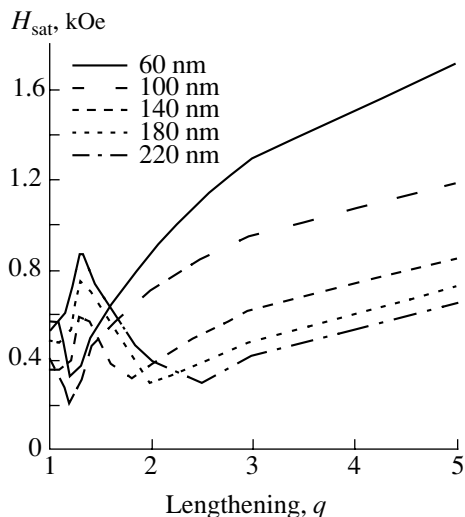


Fig. 6. Saturation field H_{sat} of magnetite particles as a function of their length-to-width ratio and size.

is eventually related to the above behavior of the effective anisotropy constant. An increase in H_c at $q > 2$ is determined by the prevailing contribution of the magnetic shape anisotropy.

A decrease in the coercive force with increasing particle size is related to their transformation to the nonuniform (quasi-single-domain, two-domain) state. Enhancement of the nonuniformity of magnetic-moment distribution in a grain favors an increase in the reversible magnetization component, which results in the above described behavior of H_c .

Note that the saturation field H_{sat} for the particles with a non-uniform distribution of magnetic moment ($a > 100$ nm, Fig. 6) achieves a maximum at $q \approx 1.3$. This can be attributed to going through the minimum of the effective anisotropy constant, since a decrease in anisotropy favors the nonuniform distribution of magnetization in a grain. An increased non-uniformity hinders the reversible magnetization processes that determine the shape of the hysteresis loop in the saturation region.

An increased prolateness of a two-domain particle may cause its transformation to the quasi-single-domain state or to the uniform state. This is accompanied by an increase in the uniformity of the magnetic moment of the grain. The role of irreversible magnetization process increases, which is reflected in the behavior of $H_{sat} = H_{sat}(q)$ at $q > 2$ (Fig. 6). The saturation field for particles that are at $H = 0$ in the single-domain state ($a = 60$ nm) or in the quasi-single-domain state ($a = 100$ nm) is equal to their coercive force (whose behavior depending on the grain size and aspect ratio was discussed above).

Figure 7 shows the dependence of H_c and switching field H_s on the angle ϕ between the long edge of the particle and the applied field direction \mathbf{H} ; H_s is the minimum critical field H_{cr} providing remanent magnetization along the \mathbf{H} direction. The introduction of this parameter is necessary to characterize the degree of irreversibility magnetization.

The coercive force of cubic particles with a uniform magnetic moment ($a = 60$ nm) in the initial state ($H = 0$) changes drastically as a function of the angle ϕ . As could be expected, upon magnetization along the easy axis ($\phi = 45^\circ$), H_c is equal to the theoretical value $H_c = 2K/I_s = 570$ Oe [21], which is due to the uniform rotation of the magnetic moment of the grain.

Larger particles ($a = 160$ nm) undergo nonuniform magnetization reversal. H_c in this case is determined by the reversible variations of magnetization and only slightly depend on ϕ . In an applied field equal to the switching field H_s , the particle transforms from the two-domain state to the quasi-single-domain state with a magnetization distribution symmetric about the easy axis. That is why H_s is minimal at $\phi = 45^\circ$.

For comparison with the results of three-dimensional simulation of magnetization of elongated maghemite ($\gamma\text{-Fe}_2\text{O}_3$) particles [8], H_c and H_s were calculated for magnetite grains with an aspect ratio $q = 6$ (Fig. 7b). The curves of the coercive force H_c and switching field H_s qualitatively follow the corresponding curves in [8], i.e., H_c decreases and H_s varies non-monotonically with increasing ϕ . Note that for small particles ($a = 60$ nm), the point of inflection of the $H_c = H_c(\phi)$ curve at $\phi = 45^\circ$ coincides with the position of the minimum in the $H_s = H_s(\phi)$ curve, whereas H_s of large grains ($a = 160$ nm) increases monotonically. The difference in the H_s behavior for the small and large

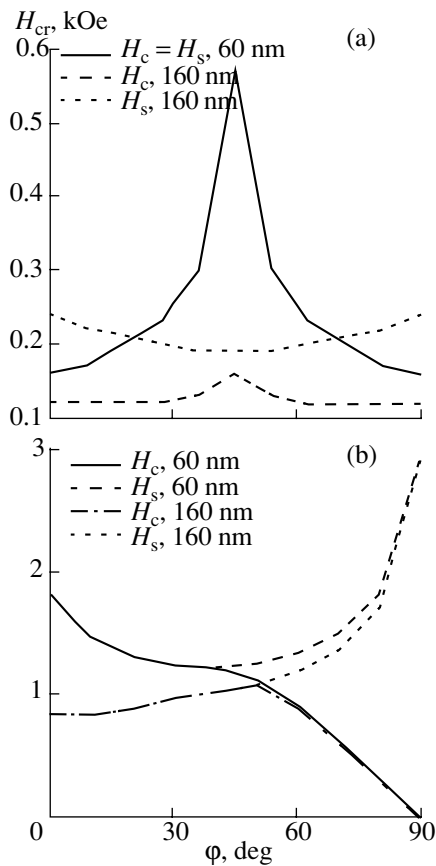


Fig. 7. Coercive force H_c and switching field H_s as functions of the angle between the longer edge of a grain and the applied magnetic field for a particle with $a = 60$ and 160 nm: (a) $q = 1$ and (b) $q = 6$.

grains is due to the uniform and nonuniform magnetization, respectively.

The qualitative agreement of the $H_c = H_c(\phi)$ and $H_s = H_s(\phi)$ curves with the corresponding curves calculated by Yan and Della Torre [8] confirms the validity of the simplified two-dimensional model used in this work and the consistency of the results obtained.

REFERENCES

1. Amar, H., Size Dependence of the Wall Characteristics in a Two-Domain Iron Particle, *J. Appl. Phys.*, 1958, vol. 29, pp. 542–543.
2. Enkin, R.J. and Dunlop, D.J., A Micromagnetic Study of Pseudo-Single-Domain Remanence in Magnetite, *J. Geophys. Res.*, 1987, vol. 92, pp. 12726–12740.
3. Williams, W. and Dunlop, D.J., Three-Dimensional Micromagnetic Modelling of Ferromagnetic Domain Structure, *Nature (London)*, 1989, vol. 337, pp. 634–637.
4. Shcherbakov, V.P., Lamash, B.E., and Shcherbakova, V.V., *Fizika magnetizma gornykh porod* (Physics of Magnetism of Rocks), Moscow: Inst. Fiziki Zemli, 1991.
5. Fabian, K., Kirchner, A., Williams, W., *et al.*, Three-Dimensional Micromagnetic Calculations for Magnetite Using FFT, *Geophys. J. Int.*, 1996, vol. 124, pp. 89–104.
6. Schabes, M.E., Micromagnetic Theory of Non-Uniform Magnetization Processes in Magnetic Recording Particles, *J. Magn. Magn. Mater.*, 1991, vol. 95, pp. 249–288.
7. Schabes, M.E. and Bertram, H.N., Magnetization Processes in Ferrimagnetic Cubes, *J. Appl. Phys.*, 1988, vol. 64, no. 3, pp. 1347–1357.
8. Ying Dong Yan and Edward Della Torre, Modeling of Fine Ferromagnetic Particles, *J. Appl. Phys.*, 1989, vol. 66, no. 1, pp. 320–327.
9. Schmidts, H.F. and Kronmüller, H., Magnetization Processes in Small Ferromagnetic Particles with Inhomogeneous Demagnetizing Field and Uniaxial Anisotropy, *J. Magn. Magn. Mater.*, 1994, vol. 129, pp. 361–377.
10. Lu Hua, Bishop, J.E.L., and Tucker, J.W., The Micromagnetics of Cubic Particles with Cubic Anisotropy Favouring Body Diagonal Magnetization, *J. Magn. Magn. Mater.*, 1994, vol. 131, pp. 285–294.
11. Dunlop, D.J., Developments in Rock Magnetism, *Rep. Prog. Phys.*, 1990, vol. 53, pp. 707–792.
12. Dunlop, D.J., Superparamagnetic and Single-Domain Threshold in Magnetite, *J. Geophys. Res.*, 1973, vol. 78, pp. 1780–1793.
13. Dunlop, D.J. and Bina, M.M., The Coercive Force Spectrum of Magnetite at High Temperatures: Evidence for Thermal Activation Below the Blocking Temperature, *Geophys. J. R. Astron. Soc.*, 1977, vol. 51, pp. 121–147.
14. Butler, R.F. and Banerjee, S.K., Theoretical Single-Domain Grain Size Range in Magnetite and Titanomagnetite, *J. Geophys. Res.*, 1975, vol. 80, pp. 4049–4058.
15. Afremov, L.L. and Belokon', V.I., Calculating the Critical Field of Single-Domain Grains of Rocks, *Izv. Akad. Nauk SSSR, Fiz. Zemli*, 1977, no. 3, pp. 104–108.
16. Afremov, L.L. and Belokon', V.I., Calculating Remanent Magnetization of a System of Single-Domain Particles, *Izv. Akad. Nauk SSSR, Fiz. Zemli*, 1979, no. 4, pp. 122–128.
17. Kondorskii, E.I., Single-Domain Structure in Ferromagnets and Magnetic Properties of Finely Dispersed Substances, *Dokl. Akad. Nauk SSSR*, 1950, vol. 70, no. 2, pp. 215–218.
18. Kondorskii, E.I., Single-Domain Structure in Ferromagnets and Magnetic Properties of Finely Dispersed Substances, *Dokl. Akad. Nauk SSSR*, 1950, vol. 74, no. 2, pp. 213–216.
19. Kondorskii, E.I., On the Theory of Single-Domain Particles, *Dokl. Akad. Nauk SSSR*, 1952, vol. 82, no. 3, pp. 365–368.
20. Aharoni, A., Magnetization Curling, *Phys. Status Solidi*, 1966, vol. 16, no. 3, pp. 3–42.
21. Stoner, E.C. and Wohlfarth, E.P., A Mechanism of Magnetic Hysteresis in Alloys, *Philos. Trans. R. Soc. A (London)*, 1948, vol. 240, p. 599.